Supplemental material

Selective, User-friendly, Highly Porous, Efficient, and Rapid (SUPER) Filter for Isolation and Analysis of Rare Tumor Cells.

Kaifeng Zhao†[a, c], Yaoping Liu†[b], Hua Wang†[a], Yanling Song[c], Xiaofeng Chen[c], Chen Huang[a], Qi Niu[a], Jiao Cao[a], Xin Chen[a], Wei Wang*[b], Lingling Wu*[b], Chaoyong Yang[a, c]

[a.] Institute of Molecular Medicine, Clinical Laboratory, Department of Gastrointestinal Surgery, Renji Hospital, Shanghai Jiao Tong University School of Medicine, Shanghai, 200127, China.
[b.] Institute of Microelectronics, Peking University, Beijing, 100871, China.
[c.] The MOE Key Laboratory of Spectrochemical Analysis & Instrumentation, the Key Laboratory of Chemical Biology of Fujian Province, State Key Laboratory of Physical Chemistry of Solid Surfaces, Collaborative Innovation Center of Chemistry for Energy Materials, Department of Chemical Biology, College of Chemistry and Chemical Engineering, Xiamen University, Xiamen 361005, China.
† These authors contributed equally.

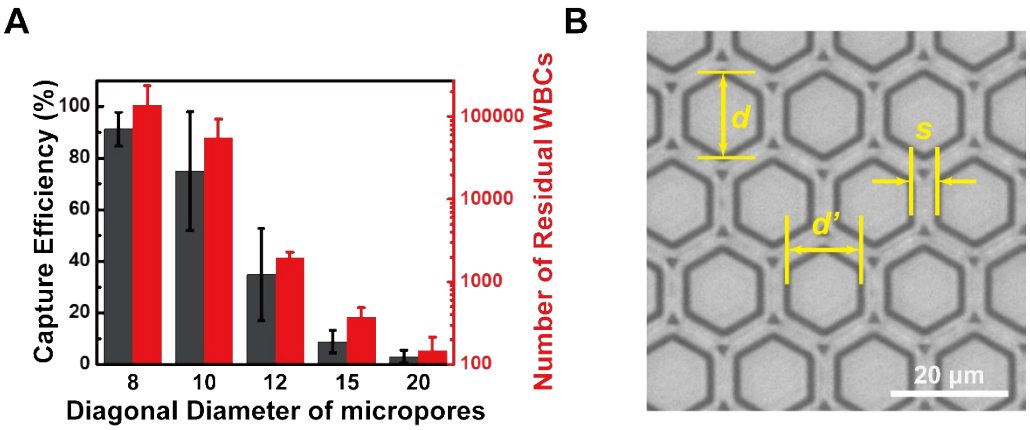

Figure S1. A) Capture efficiency and residual WBC counts of 2.5D micropore array filtration membranes with different diagonal diameters of micropores. Detailed parameters were listed in **Table S1.** Error bars represent the standard deviation of three repeat experiments. B) Illustration of key parameters of 2.5D micropore assay filtration membranes: diagonal diameter (*d*), edge-to-edge diameter (*d'*) and edge-to-edge space (*s*).

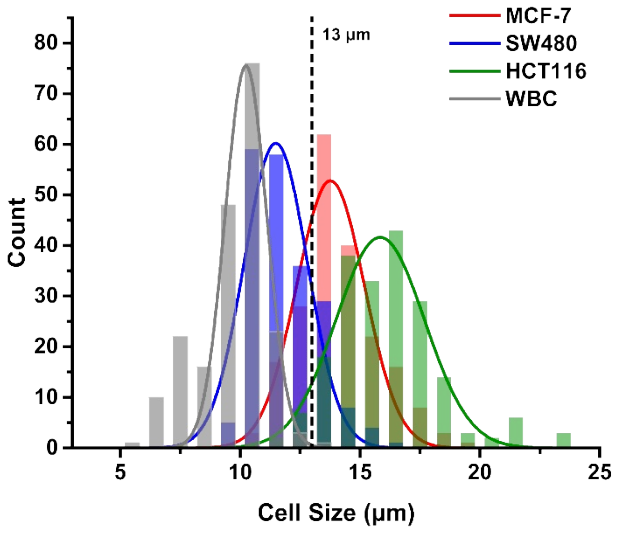

Figure S2. Cell size distribution (bars) and regression curve (line) of cells lines used in this study. The dash line indicates the approximate size of micropores on SUPER Filter.

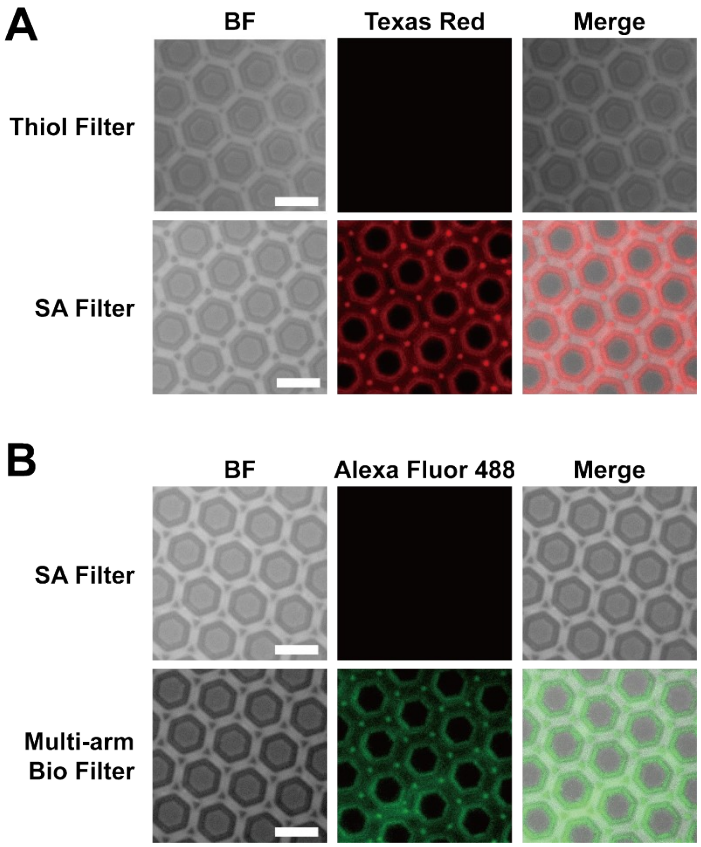

Figure S3. Fluorescence characterization of modified filtration membranes. A) Micrographs of Thiol Filter and SA Filter stained by bio-T16-Texas Red. B) Micrographs of SA Filter and Multi-arm Bio Filter stained by Alexa Fluor 488 conjugated SA. Scale bars: 10 μm.

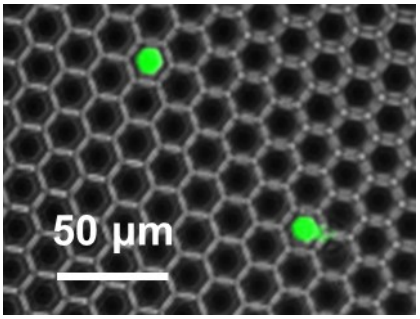

Figure S4. Fluorescence micrograph of SW480 cells (stained with Calcein-AM) captured on SUPER Filter, showing that tumor cells are smaller than the micropores on the filter.

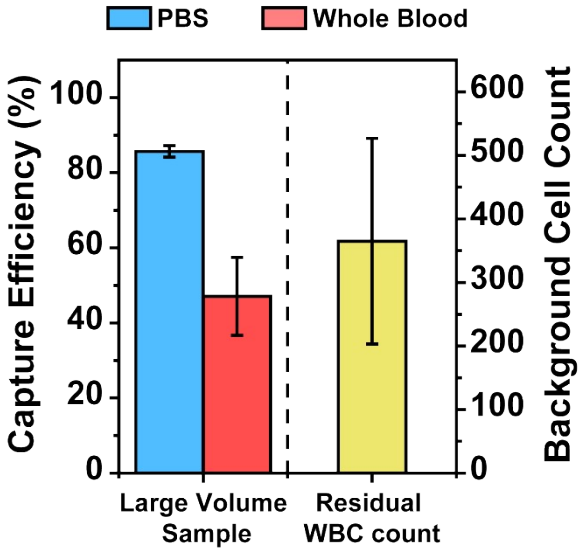

Figure S5. Capture performance of SUPER Filter towards SW480 cells in large volume samples, including capture efficiencies in PBS and whole blood (10 mL for PBS (blue) and 4 mL for whole blood (red), 20 cells/mL), and residual WBC count. Error bars represent the standard deviation of three repeat experiments. SUPER Filter had similar capture efficiency towards SW480 cells in large volume (85.7 ± 1.5%) and small volume (1 mL, 91.0 ± 6.1%, **Figure 2A**) PBS, but worse in large volume whole blood (47.1 ± 10.4%) samples than small volume samples (1 mL, 83.7 ± 6.4%, **Figure 2A**). The decrease may be attributed to increased chance of collision between background cells and captured tumor cells. Nevertheless, the residual WBC count for filtration of large volume blood sample (214-536 residual WBCs) is just slightly higher than that in small volume blood samples (55-126 residual WBCs), showing SUPER Filter's excellent ability in removing background cells.

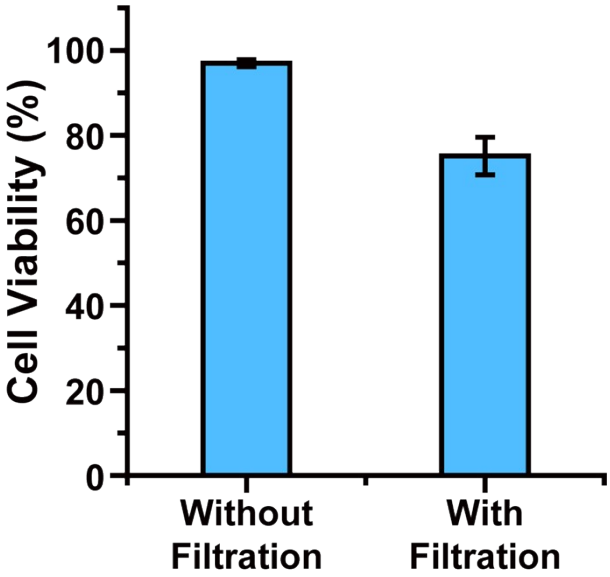

Figure S6. Viability of SW480 cells with and without affinity filtration using SUPER Filter characterized by Calcein-AM-PI staining. Error bars represent the standard deviation of three repeat experiments. The slight decrease of cell viability compared with capturing by pristine filters with 8 μm micropores (84.3 ± 5.1%)[1] could be attributed to the shear force from the fluid flowing through the gap between cell and micropore.

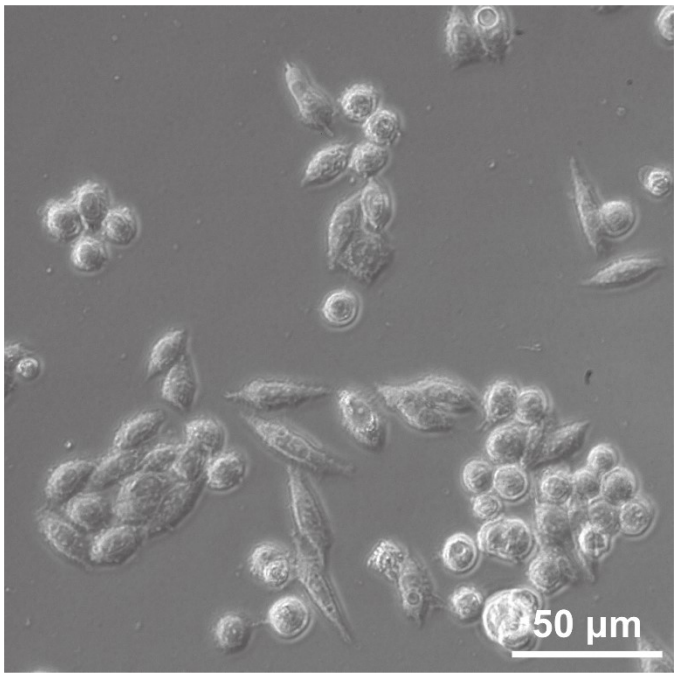

Figure S7. Phase contrast micrograph of subcultured SW480 cells from SUPER Filter one day after passage.

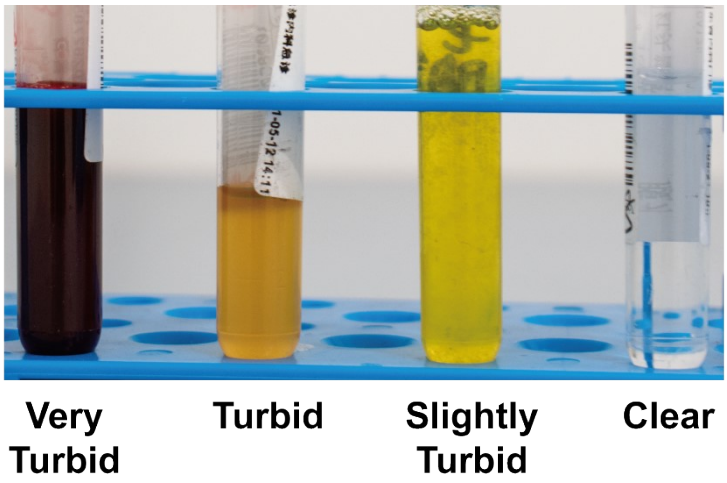

Figure S8. Examples of ascetic and pleural fluid samples with different turbidity.

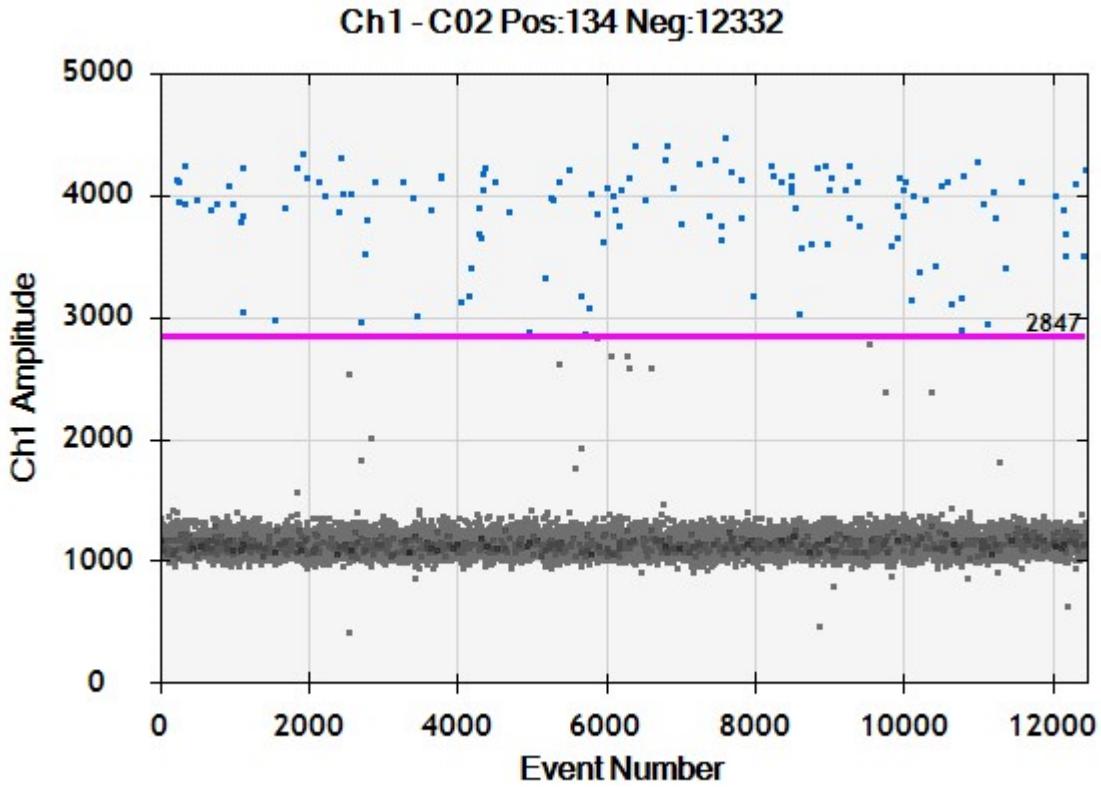

Figure S9. An example of setting the threshold for positive and negative droplets.

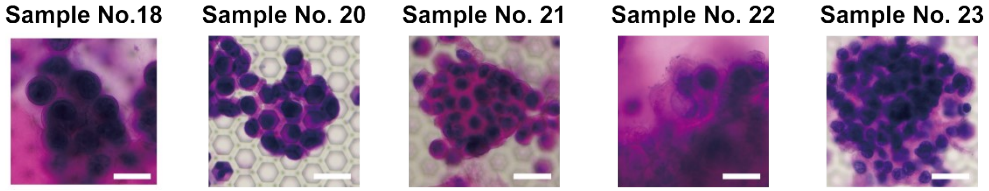

Figure S10. Representative micrographs of ETCs captured on SUPER Filter. Scale bars: 25 μm.

Table S1 Parameters of 2.5D micropore arrayed filtration membranes.

Case No.	Designed Parameters (μm)		
	d	***d'***	***s***
1	8	6.93	4
2	10	8.66	4
3	12	10.39	4
4	15	12.99	4
5	20	17.32	4
6	25	21.65	4

Table S2 Components of ddPCR reaction mixture.

Reagent	Volume/well (μL)	Final Concentration
2× ddPCR Super mix (no dUTP)	10	
Primer Mix (1:1 mixture of forward primer and reverse primer, 18 μM each)	1	900 nM
Mutant Probes (100 μM)	0.05 each	250 nM
Wild type probes (100 μM)	0.05 each	250 nM
Sample	8	
Nuclease-Free H_2O	Add up to 20 μL	

Table S3 Sequences of ddPCR primers and hydrolysis probes.

Target mutation	Forward Primer (5'-3')	Probes (5'-3') Wild Type (5'HEX, 3'MGB) Mutant (5'FAM, 3'MGB)	Reverse Primer (5'-3')
G12C	AGGCCTGCTGAAAATGACTGAATAT	CCTACGCCACCAGCT CTACGCCACAAGCT	GCTGTATCGTCAAGGCACTCT
G12A		CCTACGCCACCAGCT CTACGCCAGCAGCT	
G12D		TTGGAGCTGGTGGCGT TGGAGCTGATGGCGT	
G12S		CTACGCCACCAGCTC CTACGCCACTAGCTC	
G12V		CTACGCCACCAGCTC ACGCCAACAGCTC	
G12R		TTGGAGCTGGTGGCGT TTGGAGCTCGTGGCGT	
G13D		TGGTGGCGTAGGCA CTGGTGACGTAGGCA	

Table S4 PCR program for ddPCR.

Temperature	Time	Temperature Gradient	Cycles
95 °C	10 min		1
94 °C	30 s	2 °C/s	40
60 °C	1 min		
98 °C	10 min		1
4 °C	Infinite hold	1 °C/s	

Table S5 Summary of the present tumor cell separation technologies.

Separation Strategy	Sample Pretreatment	No. of Residual Background Cells	Reference
Immunoaffinity	Incubation with immunomagnetic beads	~1000 cells	[2]
	None	~500 cells*	[3]
Affinity filtration	1:6 dilution	<1000 cells	[4]
	1:1 dilution	~25000 cells	[5]
Filtration	None	150~300 cells	[6]
	None	>1600 cells*	[7]
	Fixation	3920 ± 1883 cells	[8]
Immunobeads assisted filtration	RBC lysis, incubation with immunomagnetic beads	Average 4016 cells	[9]
	WBC removal by anti-CD45 immunomagnetic beads	~1000 cells	[10]

* Calculated from reported purity or enrichment factor.

Table S6 Information of blood samples.

Sample No.	Sex	Age	Clinical Investigation	CTC Counts
1	Female	66	Colorectal cancer	18
2	Female	72	Gastric cancer	2
3	Male	67	Colorectal cancer and gastric cancer	3
4	Male	56	Gastric cancer	6
5	Male	74	Gastric cancer	9
6	Female	75	Breast Cancer	6
7	Male	61	Colorectal cancer	9
8	Male	58	Colorectal cancer, *KRAS* G12D/S mutation	5
9	Male	57	Colorectal cancer, *KRAS* G12D/S mutation	9
10	Female	67	Coloraectal cancer, *KRAS* G12C/R/V/A, G13D mutation	4
11	Female	50	Colorectal cancer	13
12	Male	68	Colorectal cancer	2
13	Male	41	Healthy	1
14	Male	40	Healthy	0
15	Female	37	Healthy	0
16	Female	37	Healthy	0
17	Male	40	Healthy	1

Table S7 Information of pleural fluid and ascetic fluid samples.

Sample No.	Sample Type*	Sex	Age	Sample Volume	Turbidity**	Result	Clinical Investigation
18	P	F	76	1 mL	++	Positive	Lung cancer
19	A	M	64	1 mL	++	Positive	Colorectal cancer
20	P	F	83	5 mL	++	Positive	Lung cancer
21	A	M	44	5 mL	-	Positive	Bile duct cancer
22	A	F	71	1 mL	++	Positive	Ovarian cancer
23	A	M	57	4 mL	++	Positive	Gastric cancer
24	A	M	79	5 mL	-	Negative	Type 2 diabetes
25	P	M	46	3.5 mL	+++	Negative	Nephritis
26	A	M	71	2 mL	++	Negative	Renal insufficiency
27	P	M	80	5 mL	+	Negative	Hyponatremia
28	P	M	69	5 mL	-	Negative	Hypoxemia

*: A: Ascetic fluid, P: Pleural fluid.
: -: clear, +: slightly turbid, ++: turbid, +++: very turbid, examples in **Figure S9.

References

[1] Liu, Y.; Li, T.; Xu, M.; Zhang, W.; Xiong, Y.; Nie, L.; Wang, Q.; Li, H.; Wang, W., *Lab Chip* **2018,** *19* (1), 68-78.

[2] Ozkumur, E.; Shah, A. M.; Ciciliano, J. C.; Emmink, B. L.; Miyamoto, D. T.; Brachtel, E.; Yu, M.; Chen, P.-i.; Morgan, B.; Trautwein, J.; Kimura, A.; Sengupta, S.; Stott, S. L.; Karabacak, N. M.; Barber, T. A.; Walsh, J. R.; Smith, K.; Spuhler, P. S.; Sullivan, J. P.; Lee, R. J.; Ting, D. T.; Luo, X.; Shaw, A. T.; Bardia, A.; Sequist, L. V.; Louis, D. N.; Maheswaran, S.; Kapur, R.; Haber, D. A.; Toner, M., *Sci. Trans. Med.* **2013,** *5* (179), 179ra47.

[3] Stott, S. L.; Hsu, C. H.; Tsukrov, D. I.; Yu, M.; Miyamoto, D. T.; Waltman, B. A.; Rothenberg, S. M.; Shah, A. M.; Smas, M. E.; Korir, G. K.; Floyd, F. P., Jr.; Gilman, A. J.; Lord, J. B.; Winokur, D.; Springer, S.; Irimia, D.; Nagrath, S.; Sequist, L. V.; Lee, R. J.; Isselbacher, K. J.; Maheswaran, S.; Haber, D. A.; Toner, M., *Proc. Natl. Acad. Sci. U. S. A.* **2010,** *107* (43), 18392-18397.

[4] Meunier, A.; Hernandez-Castro, J. A.; Turner, K.; Li, K.; Veres, T.; Juncker, D., *Anal. Chem.* **2016,** *88* (17), 8510-8517.

[5] Chen, K.; Dopico, P.; Varillas, J.; Zhang, J.; George, T. J.; Fan, Z. H., *Angew. Chem. Int. Ed.* **2019,** *58* (23), 7606-7610.

[6] Yin, J.; Mou, L.; Yang, M.; Zou, W.; Du, C.; Zhang, W.; Jiang, X., *Anal. Chim. Acta* **2019,** *1060*, 133-141.

[7] Zhou, M. D.; Hao, S.; Williams, A. J.; Harouaka, R. A.; Schrand, B.; Rawal, S.; Ao, Z.; Brenneman, R.; Gilboa, E.; Lu, B.; Wang, S.; Zhu, J.; Datar, R.; Cote, R.; Tai, Y. C.; Zheng, S. Y., *Sci. Rep.* **2014,** *4*, 7392.

[8] Adams, D. L.; Zhu, P.; Makarova, O. V.; Martin, S. S.; Charpentier, M.; Chumsri, S.; Li, S.; Amstutz, P.; Tang, C. M., *RSC Adv.* **2014,** *9*, 4334-4342.

[9] Chang, C. L.; Huang, W.; Jalal, S. I.; Chan, B. D.; Mahmood, A.; Shahda, S.; O'Neil, B. H.; Matei, D. E.; Savran, C. A., *Lab Chip* **2015,** *15* (7), 1677-1688.

[10] Sun, N.; Li, X.; Wang, Z.; Li, Y.; Pei, R., *Biosens. Bioelectron.* **2018,** *102*, 157-163.